ACS Sustainable Chemistry & Engineering

Research Article

pubs.acs.org/journal/ascecg

Activated Carbons Derived from Hydrothermally Carbonized Sucrose: Remarkable Adsorbents for Adsorptive Desulfurization

Yawei Shi, Xiangwen Zhang,* and Guozhu Liu*

Key Laboratory for Green Chemical Technology of Ministry of Education, School of Chemical Engineering and Technology, Collaborative Innovation Center of Chemical Science and Engineering (Tianjin), Tianjin University, Tianjin 300072, China

Supporting Information

ABSTRACT: Activated carbons derived from hydrothermal carbonization of sucrose and subsequent KOH activation have been prepared and tested for the adsorptive removal of refractory thiophenic compounds. Textural and chemical properties of the carbons and their corresponding impacts on adsorption rates and capacities were discussed in detail. The optimum carbon possessed high adsorption capacity (41.5 mgS/g for 300 ppmwS model oil), fast adsorption rate (97% saturated within 5 min) as well as relatively good selectivity for the adsorption of thiophenic compounds due to the abundant small micropores, suitable mesopore fraction and various oxygen functionalities present in the carbon. Combined with the economic and environmental merits of the preparation procedure, the sucrose-derived activated carbons are promising candidates for potential practical applications.

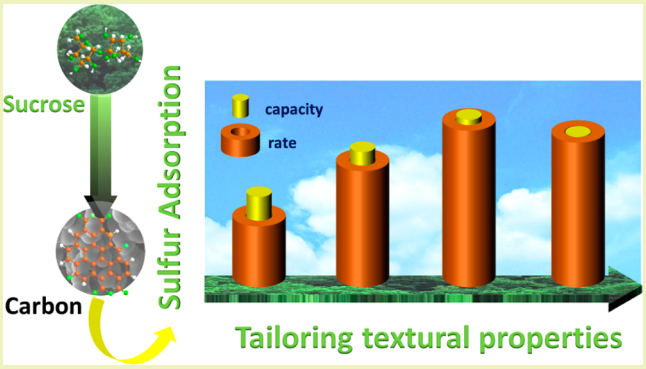

KEYWORDS: *Sucrose, Activated carbon, Adsorption, Desulfurization, Dibenzothiophene*

INTRODUCTION

Sulfur compounds, which are naturally present in fuels, are released to the atmosphere as toxic sulfur dioxide, causing significant environmental and health problems.[1−3] To reduce the sulfur content in fuels, the traditional hydrodesulfurization (HDS) process is widely employed. Despite that HDS performs well in the removal of thiols, sulfides and disulfides, it faces some major problems, such as resistance to thiophenic compounds as well as high energy and hydrogen consumptions.[4,5] Consequently, a series of alternative technologies have been developed, among which adsorptive desulfurization (ADS) is considered as a promising approach with several advantages, including mild operating conditions and selective removal of refractory thiophenic compounds.[6−8]

Various adsorbents have been investigated in the ADS process, such as ion-exchanged zeolites,[6,9] metal oxides,[10−13] metal−organic frameworks (MOFs)[4,14,15] and carbon-based materials.[5,16−25] Among these adsorbents, carbon-based materials have gained much attention due to their controllable textural and chemical properties. Commercial activated carbons,[18,26−28] homemade activated carbons[16,17,29,30] and also some advanced carbon-based materials, including graphene,[31,32] ordered mesoporous carbons[33,34] and MOF-derived carbons,[20] have been applied in the ADS process. However, the ADS performances of commercial activated carbons are not that satisfactory. On the other hand, most of the homemade activated carbons or advanced carbon-based materials applied in ADS are derived from fossil-based precursors and/or suffer from complex preparation procedures, which may hinder their potential industrial applications. In this regard, the preparations of ADS adsorbents from cheap precursors, including polyethyleneterephthalate waste,[35] rice hull,[25] and sewage sludge,[36] have been reported by some researchers. However, a preset high temperature carbonization step before activation is generally applied in these processes, leading to additional cost.

Recently, the synthesis of carbon materials from the hydrothermal carbonization (HTC) of pure carbohydrates as well as raw lignocellulosic biomass is attracting increasing attention.[37−45] As a typical disaccharide, sucrose has been hydrothermally treated by numerous groups. In 2001, Wang et al. employed the hydrothermal treatment of sucrose to produce carbonaceous microspheres.[43] Later on, Titirici et al.,[46] Sevilla et al.,[47] Falco et al.[48] and Romero-Anaya et al.[39] systematically investigated the effect of different experimental conditions and characterized the chemical and structural properties of the resulting sucrose-derived carbons produced by HTC. Because of the utilization of cheap natural precursors and low carbonization temperatures, this approach is considered as a green and economic one.

However, one limitation of the carbons produced by HTC is that they possess little porosity. Generally, to develop the pore network in carbon materials, either physical or chemical

Received: June 9, 2015
Revised: August 4, 2015
Published: August 7, 2015

DOI: 10.1021/acssuschemeng.5b00670
ACS Sustainable Chem. Eng. 2015, 3, 2237−2246

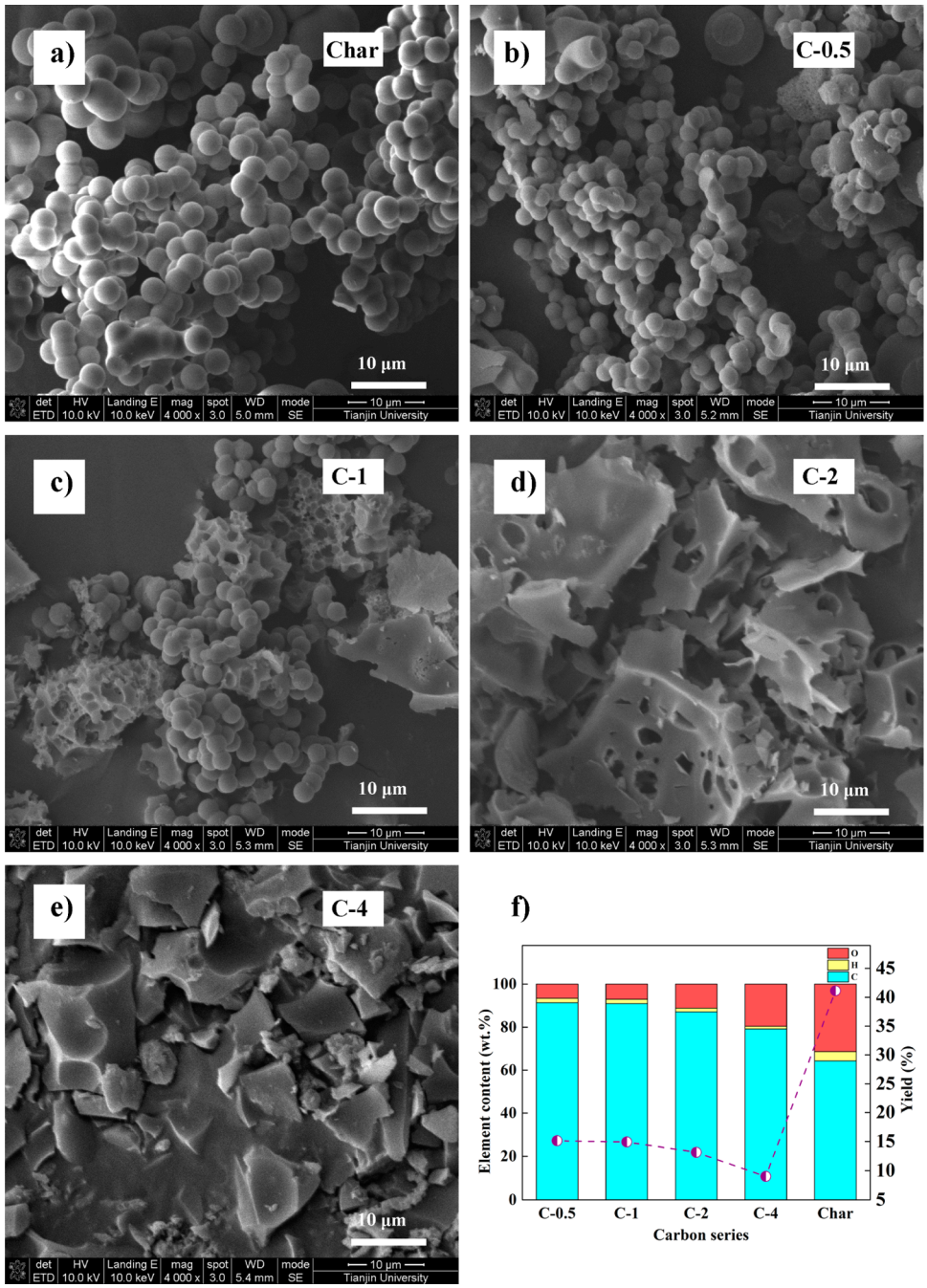

Figure 1. SEM images (a–e) and elemental contents and yields (f) of the carbon samples.

activation is required.[49] Compared to physical activation, chemical activation is more advantageous considering the lower activation temperature, less activation time, as well as higher resulting surface area and pore volume.[49] Among various chemical activation methods with KOH, $ZnCl_2$, or H_3PO_4, etc., KOH activation invented in the 1970s[50] is a well-known one because it can result in activated carbons with defined micropore size distribution, high micropore volumes and large specific surface areas. Notably, this approach has been employed for the production of activated carbons produced by HTC with high surface areas and narrow micropore size distributions,[38−40,51−54] inducing noticeable applications such as methane storage,[38] hydrogen storage[40] and CO_2 capture.[51] Inspired by these encouraging results, we decided to explore the potential application in the ADS process by carefully tailoring the textural and chemical properties of the activated carbons produced by HTC, which has not been reported until now. Because the ADS process is considered a sustainable one due to the mild operating conditions, the introduction of the sustainable carbons produced by HTC into ADS may make the whole process more sustainable.

In the present work, sustainable activated carbons with abundant small micropores and suitable mesopore fractions prepared by hydrothermal treatment of sucrose and subsequent KOH activation have been utilized in the ADS process. The optimum activated carbon possessed a fast adsorption rate (97% saturated within 5 min), high adsorption capacity (41.5 mgS/g for 300 ppmwS model oil) as well as relatively good selectivity for

DOI: 10.1021/acssuschemeng.5b00670
ACS Sustainable Chem. Eng. 2015, 3, 2237−2246

the adsorption of thiophenic compounds. Combined with their economic and environmental merits, these sucrose-derived activated carbons are promising candidates for ADS from academic, industrial and environmental viewpoints.

EXPERIMENTAL SECTION

Preparation. The synthesis of activated carbons comprised two steps: (a) HTC of sucrose at 180 °C and (b) chemical activation with KOH. In a typical synthesis, 5.4768 g of sucrose (AR, Tianjin Guangfu Chemical Industry, Tianjin, China) was dissolved in 20 mL of distilled water and put into a 50 mL capacity Teflon-lined stainless steel autoclave in an oven preheated to 180 °C. After 24 h, the solid product was recovered by filtration, washed with distilled water for three times and dried in an over at 120 °C overnight. A comparison of HTC conditions with previous reports can be found in Table S1 in the Supporting Information. For chemical activation, the resulting char was mixed with KOH (90%, Aladdin, China) in a mass ratio of 1:0.5, 1:1, 1:2 or 1:4, heated at 750 °C for 1 h in nitrogen atmosphere in a horizontal quartz furnace tube, and washed with distilled water to constant pH. The resulting carbon prepared at the char/KOH ratio of 1:x was denoted as C-x.

Characterization. The morphologies of the samples were characterized by scanning electron microscopy (SEM, FEI, Nanosem 430 field emission gun scanning electron microscope). Fourier transform infrared (FTIR) spectra of the samples were recorded using a Bruker Vertex 70 IR spectrometer (4 cm^{-1}) in KBr media. CHN elemental analysis was performed on a Vario EL CUBE elemental analyzer. Pore characteristics of the materials were assessed from nitrogen adsorption−desorption isotherms measured at −196 °C on a Micromeritics ASAP 2020. The specific surface area (S_{BET}) was calculated from the Brunauer−Emmett−Teller (BET) method in the relative pressure range selected based on the rules established by Rouquerol et al.[55] An example and corresponding detailed discussions (Figure S1 and Table S2) are shown in the Supporting Information. For the pore size distribution, the volume of micropores (V_{micro}) and the volume of pores smaller than 1 nm ($V_{<1\ nm}$), the nonlocal density functional theory (NL-DFT) method was used and assuming a slit pore model. The total pore volume (V_t) was calculated from the last point on the isotherm, and the mesopore volume (V_{meso}) was calculated from the difference between V_t and V_{micro}.

Adsorption Experiments. Model oils were prepared by dissolving appropriate amounts of benzothiophene (BT), dibenzothiophene (DBT) or 4,6-dimethyldibenzothiophene (DMDBT) into *n*-octane or mixtures of *n*-octane and *para*-xylene. BT (98%) and DBT (98%) were purchased from J&K Chemical Ltd. (Beijing, China). DMDBT (98%) was purchased from Sinopharm Chemical Reagent Co., Ltd. (Beijing, China), whereas *n*-octane (98%) and *para*-xylene (99%) were obtained from Tianjin Jiangtian Chemical Industry (Tianjin, China). The initial sulfur concentration was 100 ppmwS within experimental error in all experiments unless otherwise stated.

Before adsorption, carbon materials were degassed overnight at 120 °C. An appropriate amount of carbon was added into a glass flask with a magnetic stirrer. Then the model oil (25 mL) was added, and the mixture was stirred for a desired time at 25 °C in a water bath for an appropriate time. After that, the solution was separated from the adsorbent with a syringe filter (hydrophobic, 0.22 μm), and the sulfur concentration was measured. The sulfur content was analyzed with an elemental analyzer (Analytical jena, multi EA 5000). All the adsorption experiments were performed twice to give an average.

The amount of sulfur adsorbed (q_t) by the carbon was calculated using eq 1:

$$q_t = (C_0 - C_t)V/W \quad (1)$$

where C_0 and C_t (mgS/L) are the liquid-phase sulfur concentration at times = 0 and t, respectively. V (mL) and W (mg) are the volume of the model oil and the weight of the adsorbent, respectively.

Sulfur removal (%) was calculated using eq 2:

$$\text{sulfur removal}\ (\%) = 100(C_0 - C_e)/C_0 \quad (2)$$

RESULTS AND DISCUSSION

Characterizations of the Adsorbents. The morphologies of the char and the activated carbons characterized by SEM are illustrated in Figure 1. Microspheres, which are the typical morphologies of carbohydrate-derived chars produced by HTC,[38,39] were developed after hydrothermal treatment (Figure 1a). The spherical chars suffered changes in their morphologies depending on the char/KOH ratio (1:x) after chemical activation (Figure 1b−e). With the lowest KOH amount (x = 0.5), most of the particles maintained the spherical morphology with a shrinkage in the size (Figure 1b). With a larger KOH amount (x = 1), only part of the spheres remained intact, whereas some large-sized fragments with sharp edges were formed (Figure 1c). Further increasing the KOH amount resulted in the formation of more large fragments at the expense of complete disappearance of spheres particles (Figure 1d,e).

During the KOH activation process, redox reactions that take place between various potassium compounds and the carbon are responsible for the generation of the pore network.[40,49,56] The formation of H_2O and CO_2 also contributes to the further development of the porosity through the gasification of carbon.[49,57,58] In addition, the vapors of as-prepared metallic K are intercalated between the carbon lattices, causing swelling and disruption of the carbon microstructure.[49,59] With increasing amounts of KOH in the activation process, all these effects became stronger, leading to more drastic morphology evolutions. This is also reflected in the yield decline with increasing KOH amounts. As is shown in Figure 1f, the yield based on sucrose dropped from 15.1% to 9.0% when the char/KOH ratio was increased from 0.5 to 4, indicating higher burnoff caused by more severe framework etching.

Figure 1f displays the elemental compositions of the char and activated carbons determined by CHN elemental analysis. The elemental compositions of the char in this work are similar to previously reported sucrose-derived chars produced by HTC (see Table S1 in the Supporting Information). The char possessed an oxygen content of 31.4 wt %, indicating a high concentration of oxygen-containing groups present in it. Note that the oxygen content of the sucrose precursor is 51.5 wt % based on its molecular formula ($C_{12}H_{22}O_{11}$). The drop in the oxygen content is attributed to the polymerization and carbonization processes occurred in the hydrothermal process, during which various reactions such as dehydration led to a decreased number of functional groups.[37,40] When it comes to the activated samples, the oxygen contents decreased compared to the char in all cases (Figure 1f) due to further carbonization as well as decomposition of oxygen-containing functional groups at a high temperature.[40,60] On the other hand, the oxygen contents increased while the carbon contents dropped with larger KOH/char ratios, again proving that more carbon atoms were oxidized into CO/CO_2 and released into the gas phase, in accordance with the changes in morphologies and yields.

FTIR measurements were further performed to investigate the surface functionalities of the samples (Figure 2). A broad absorption centered at 3400 cm^{-1} is assigned to O—H stretching in water,[61] whereas the bands at around 1700, 1580 and 1100 cm^{-1} are assigned to C═O, C—C and C—O stretching vibrations, respectively.[24,62] Despite that these bands can be observed for both the char and the activated carbons, the intensities of most oxygen-containing bands are relatively lower for the activated ones, and the C═C stretching band shows a slight shift after activation. Moreover, some additional peaks can be observed for the char only, including a band at around 2925

DOI: 10.1021/acssuschemeng.5b00670
ACS Sustainable Chem. Eng. 2015, 3, 2237−2246

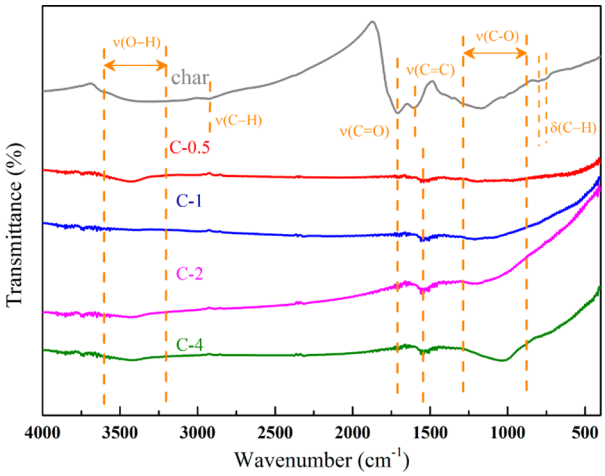

Figure 2. FTIR spectra of the carbon samples.

cm^{-1} attributed to C—H stretching mode[62] and two bands at 800 and 745 cm^{-1} probably due to C—H out-of-plane bending vibrations.[40] All these differences may be ascribed to further condensation reactions toward a more aromatic structure at a high temperature.[62]

The nitrogen adsorption−desorption isotherms and the corresponding NLDFT pore size distributions (PSDs) are plotted in Figure 3. Textural properties of the samples are summarized in Table 1. The lack of porosity in chars produced by HTC is commonly reported.[38,40,41] In our work, the char possesses limited pore volume (0.003 cm^3/g) and very low surface area (3 m^2/g), consistent with these reports. In addition, all the pores are in the mesoporous range probably attributed to interparticle voids.[40] After activation, the porosity is greatly enhanced. As is seen in Figure 3a, Type I isotherms are observed for all the activated samples, implying the microporous character of the carbons. With increasing KOH amount, the adsorption uptake at relative pressure close to 0 becomes higher and higher, indicating the formation of more micropores. In addition, a significant widening of the knee of the isotherm is observed for C-4 compared to the other samples, which implies a broadening of the micropore size range and the formation of relatively larger micorpores.[40,63] This is also confirmed by the PSD curves. As illustrated in Figure 3b, an obvious shift toward larger pore sizes is observed for C-4, whereas the other samples possess pore systems centered at similar sizes.

It is widely accepted that both textural and chemical factors are important in the ADS process. For textural properties, the volume of small micropores ($V_{<1\ nm}$) is considered as a determining factor affecting the adsorption capacity,[17,30] whereas the amount of mesopores is important for the diffusion of sulfur compounds into the micropore region.[29] In the activation process, both pore creation and pore widening may take place.[64,65] Small micropores are generated in the former case whereas larger micropores and/or mesopores are formed in the latter one through etching of the walls of already created pores. At KOH/char ratios less than 2, the effect of pore creation was dominating, resulting in increased volume of small micropores. Thus, an increase in $V_{<1\ nm}$ is observed (Table 1). In contrast, the effect of pore widening only triggered a slight shift toward larger pores sizes in the PSD as indicated in Figure 3b. This is also reflected in the ratio of $V_{<1\ nm}/V_{micro}$, which decreased slightly from 0.860 to 0.780 when the KOH/char ratio was increased from 0.5 to 2. However, a further increase from 2 to 4 resulted in

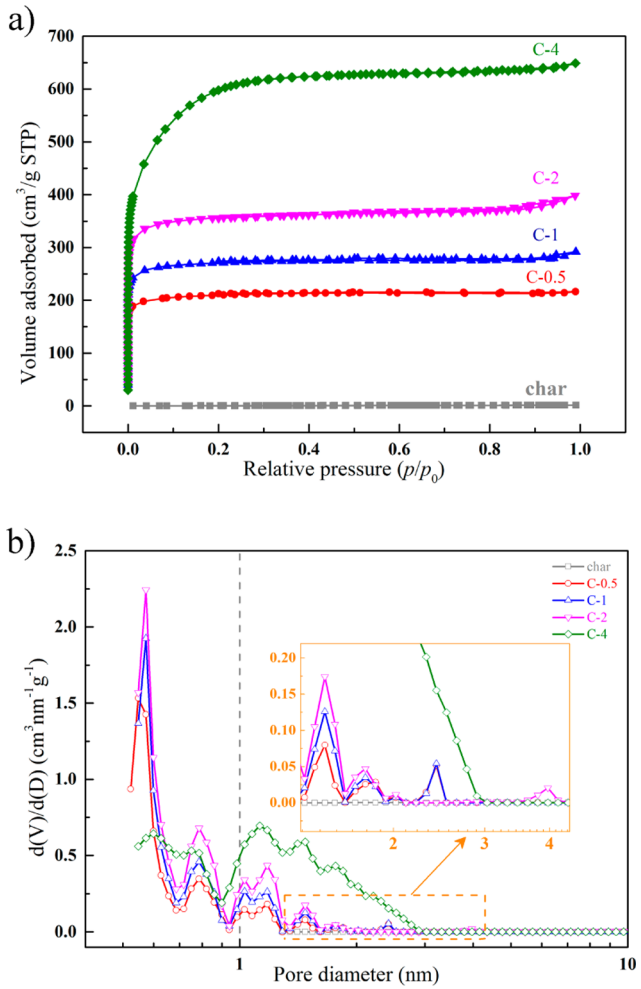

Figure 3. Nitrogen adsorption−desorption isotherms (a) and the corresponding NL-DFT pore size distributions (b) of the samples.

a decline in $V_{<1\ nm}$, and $V_{<1\ nm}/V_{micro}$ dropped dramatically to 0.386. In this situation, the effect of pore widening became dominant, and larger micropores were formed at the expense of small micropores. When it comes to V_{meso}, an increase is observed in the whole KOH/char ratio range. This is easy to understand because the effect of pore widening always takes place, leading to the formation of more mesopores.

Kinetic Study. The effect of contact time on sulfur adsorption amounts was investigated in the range of 5−120 min, and the results are presented in Figure 4. When the char was used as the adsorbent, the sulfur concentration in the model fuel remained the same as the initial one in the whole time range (data not shown). For the activated samples, different adsorption amounts were observed depending on the contact time and KOH/char ratio.

To gain a better insight into the adsorption process, the pseudo-second-order kinetic model has been used to fit the experimental data,[21,34] which is expressed by the following equation:

$$q_t = q_e^2 \cdot k_2 \cdot t/(1 + q_e \cdot k_2 \cdot t) \quad (3)$$

where q_e (mgS/g adsorbent) is the amount adsorbed at equilibrium; q_t (mgS/g adsorbent) is the amount adsorbed at contact time t (min); k_2 (g/(mg·min)) is the pseudo-second-order rate constant. The fitted curves are displayed in Figure 4

DOI: 10.1021/acssuschemeng.5b00670
ACS Sustainable Chem. Eng. 2015, 3, 2237−2246

Table 1. Texture Properties of the Char and the Activated Carbons

sample	S_{BET} [a]	V_t [b]	V_{micro} [b]	V_{meso} [b]	$V_{<1\ nm}$ [b]	$V_{<1\ nm}/V_{micro}$	V_{meso}/V_t
char	3	0.003	0.000	0.003	0.000		1.000
C-0.5	841	0.336	0.307	0.029	0.264	0.860	0.085
C-1	1088	0.453	0.408	0.045	0.327	0.800	0.099
C-2	1430	0.618	0.516	0.101	0.404	0.782	0.164
C-4	2217	1.006	0.776	0.230	0.299	0.386	0.229

[a]Measured in $m^2\ g^{-1}$. [b]Measured in $cm^3\ g^{-1}$.

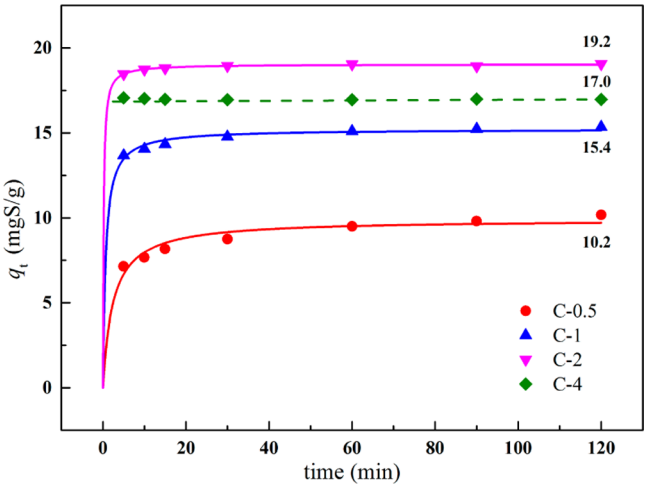

Figure 4. Kinetic studies for DBT adsorption over the carbon samples (initial sulfur concentration: 100 ppmwS DBT, T = 25 °C, adsorbent dosage = 2 g/L, no *para*-xylene added).

and the calculated parameters are listed in Table 2. Note that for C-4 the fitting failed because the adsorption amounts remained

Table 2. Pseudo-Second-Order Kinetic Model for DBT Adsorption on the Samples

sample	q_e (mgS g^{-1})	k_2 (g $mgS^{-1}\ min^{-1}$)	q_S/q_e	R^2
char	0.0			
C-0.5	9.9	0.041	0.721	0.987
C-1	15.2	0.100	0.898	0.999
C-2	19.0	0.330	0.970	0.999
C-4	17.0		1.004	

intact in the whole time range, indicating a very fast adsorption rate. As is shown in Table 2, the high regression coefficient (R^2) values showed that the ADS process in this work matched the pseudo-second-order kinetic model very well. The equilibrium adsorption amounts followed the order C-2 > C-4 > C-1 > C-0.5, and the rate constants were in the order of C-4 > C-2 > C-1 > C-0.5 (C-4 is added for clarity).

To reach equilibrium in the batch adsorption experiment, a long contact time ranging from a few hours to several days is usually employed,[5,10,16,24] leading to more operation cost from a practical viewpoint. Thus, it is highly desirable to develop ADS adsorbents with both large sulfur capacity and high adsorption rate. In this work, the order in rate constants is exactly the same as the order in mesopore fraction (V_{meso}/V_t) shown in Table 1. Obviously, the presence of more mesopores in the carbon adsorbents favored the diffusion of DBT, leading to larger rate constants. In fixed-bed adsorption systems, a contact time of several minutes is often utilized.[66,67] In this regard, we further calculated the ratios of q_S/q_e for the activated carbons. For C-0.5, q_S/q_t is only 0.721, indicating strong diffusion resistance due to the low mesopore amount (0.029 $cm^3\ g^{-1}$). In contrast, q_S/q_e reaches a high value of 0.970 for C-2 with a mesopore amount of 0.100 $cm^3\ g^{-1}$. When it comes to C-4, which has the largest mesopore fraction, the adsorption amount at 5 min is found to be equal to the value at equilibrium. Thus, for C-2 and C-4, a short contact time may be enough for fixed-bed applications. Combined with their high sulfur capacity, C-2 and C-4 are considered as promising ADS adsorbents.

Effect of Textural and Chemical Properties on Sulfur Capacity. To illustrate the effect of textural properties, q_e was plotted to the corresponding $V_{<1\ nm}$. Linear correlation showed that a good linear trend (R^2 = 0.936) existed between q_e and $V_{<1\ nm}$ (Figure 5a). This provided some strong evidence that the

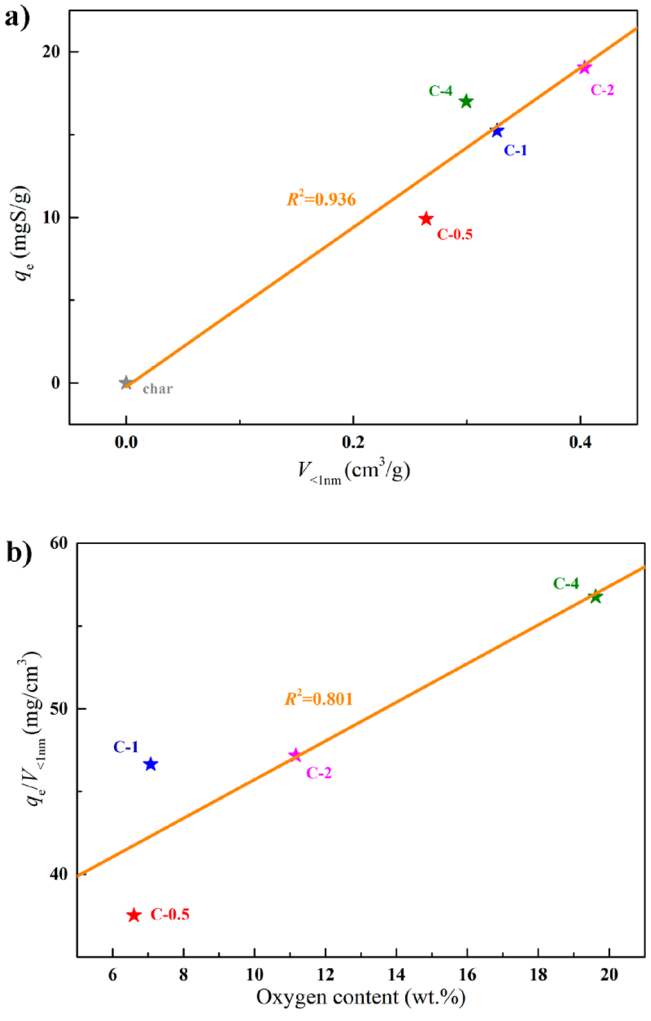

Figure 5. Effects of $V_{<1\ nm}$ (a) and oxygen content (b) on adsorption amounts.

DOI: 10.1021/acssuschemeng.5b00670
ACS Sustainable Chem. Eng. 2015, 3, 2237−2246

sulfur capacity is closely related to the amount of small micropores, in accordance with previous reports.[17,21,30] These small pores are considered be the most active adsorption centers due to the similarity of their sizes to that of DBT.[30,68]

However, compared to the values in previous reports,[17,30,68] the regression coefficient of 0.936 is relatively lower. In addition, despite that C-1 has more pores less than 1 nm compared to C-4, the order in q_e is reversed. As discussed above, with a change in the KOH amount, both textural and chemical properties of the carbons varied, the latter has been proved to have some beneficial effect on the sulfur adsorption amounts.[23−25,27,69,70] In these reports, oxidation modification of the carbons is often employed with various oxidation agents, and the increase in sulfur adsorption amount is mainly attributed to an increase of the oxygen-containing functionalities on the carbon surface.

Thus, we further evaluated the effect of chemical properties by plotting the amounts adsorbed per volume in pores smaller than 1 nm ($q_e/V_{<1\ nm}$) to the corresponding oxygen contents for the activated carbons (Figure 5b). The result showed that $q_e/V_{<1\ nm}$ increased with increasing oxygen content, which demonstrated the beneficial effect of oxygen-containing functionalities on sulfur adsorption amounts. Some specific interactions, such as acid−base interactions and polar−polar interactions may exist between the surface functionalities on the carbon surface and the sulfur atom in thiophenic compounds, favoring the adsorption of DBT in our work.

Effect of Arenes. As arenes are naturally contained in fuels, effective adsorption of thiophenic compounds in the presence of arenes is a most important issue.[23,71] The adsorptive removal of DBT in the presence of *para*-xylene has been carried out using C-2 as the adsorbent. Figure 6 shows that the adsorption amounts decreased due to the competitive adsorption of DBT and *para*-xylene.[72] With 10% *para*-xylene added (*para*-xylene:*n*-octane = 1:9 by mass), q_e decreased by 17%−44% depending on the adsorbent dosage. When the fraction of *para*-xylene was increased to 20% (*para*-xylene:*n*-octane = 2:8 by mass), a larger drop of 28%−54% in q_e was observed. For comparison, the reduction in DBT adsorption amount over a commercial activated carbon was reported to be 80% when 20% benzene was added.[19] In another work,[71] using few-layer graphene-like boron nitride as the adsorbent, the reduction was reported to be 23% with 20% *para*-xylene in the model fuel.

The divergence may be attributed to different adsorption mechanisms in different cases. Adsorption of DBT on commercial activated carbons, which has few oxygen-containing functionalities, is governed by the dispersion interactions in the small micropores through the $\pi-\pi$ interaction between the aromatic structure of DBT and the π band of the graphitic planes in the carbons.[18,35] This type of interaction also exists between the arenes and the carbons, and the dynamic diameters of the arenes (0.58 nm for benzene[73] and 0.59 nm for *para*-xylene[74]) are similar to that of DBT (0.55 nm[75]). These similarities may lead to strong competitive adsorption between DBT and arenes, resulting in significant reduction when arenes were added. In our work, the rich oxygen-containing functionalities in C-2 may act as polar[76] and/or acid centers[27] on the carbon surface, favoring DBT adsorption through specific interactions (polar−polar interaction and/or acid−base interaction) which are weak or absent between arenes and the carbon. Thus, the reduction in q_e is not that significant. Finally, in the case of boron nitride,[71] the adsorption of DBT was mainly through Lewis acid−base interaction, leading to the relatively higher selectivity for thiophenic compounds.

Adsorption Isotherms. It has been revealed above that C-2 can act as an efficient adsorbent for the adsorption of DBT. To investigate the adsorption effects of other refractory thiophenic compounds, further experiments have been performed using other adsorbates. The adsorption isotherms (Figure 7) for the three compounds (BT, DBT and DMDBT) are plotted to follow the Langmuir and Freundlich equations[34,71] and the fitting parameters are summarized in Table 3.

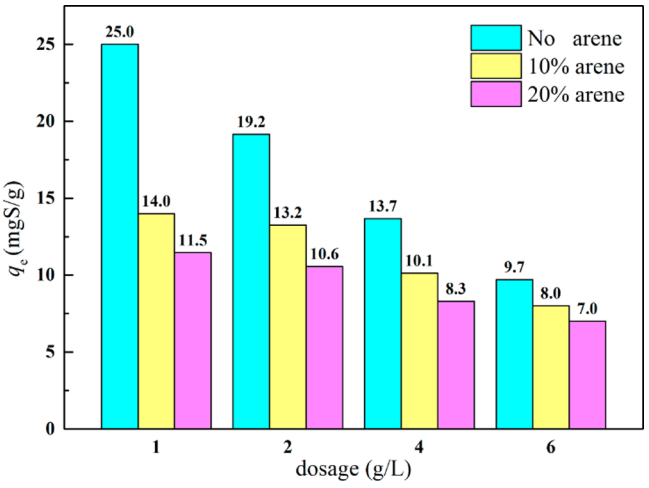

Figure 6. Effect of arenes on adsorption amounts (initial sulfur concentration: 100 ppmwS DBT, T = 25 °C, adsorbent dosage = 2 g/L; initial concentrations of *para*-xylene: 0, 10% or 20% of the model fuel).

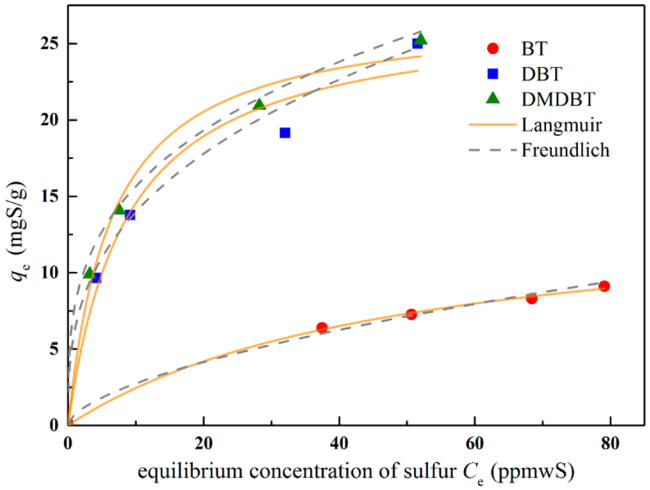

Figure 7. Adsorption isotherms for sulfur over C-2 (initial sulfur concentration: 100 ppmwS DBT, T = 25 °C, adsorbent dosage = 1−6 g/L, no *para*-xylene added).

The Langmuir equation is given as

$$q_e = q_{max} \cdot K_L \cdot C_e / (1 + C_e \cdot K_L) \quad (4)$$

where K_L (kg/mg) represents the Langmuir constant that relates to the affinity of the binding sites describing the intensity of the adsorption process, and q_{max} (mgS/g) is the maximum adsorption capacity.

The Freundlich equation can be represented as

DOI: 10.1021/acssuschemeng.5b00670
ACS Sustainable Chem. Eng. 2015, 3, 2237−2246

Table 3. Summary of Parameters from Fitting the Isotherm to Different Models

adsorbate, C_0 (mgS/kg)	Langmuir			Freundlich		
	q_{max} (mgS/g)	K_L[a]	R^2	K_F[b]	n	R^2
BT/100	14.6	0.020	0.998	0.70	1.69	0.990
DBT/100	27.0	0.116	0.968	6.27	2.87	0.955
DMDBT/100	27.2	0.155	0.988	7.80	3.30	0.940

[a]Measured in kg mgS^{-1}. [b]Measured in (mgS g^{-1}) (kg $mgS^{-1})^{1/n}$.

$$q_e = K_F \cdot C_e^{1/n} \quad (5)$$

where K_F and n are Freundlich constants indicative of adsorption capacity and adsorption intensity, respectively.

As is shown in Table 3, the correlation coefficients for the Langmuir model were larger than those for the Freundlich model, suggesting that the Langmuir model was slightly more suitable for the carbons. The maximum adsorption capacities (q_{max}) calculated by the Langmuir model are 14.6, 27.0 and 27.2 mgS/g for BT, DBT and DMDBT, respectively. The order of DMDBT > DBT > BT is in accordance with previous reports,[77−82] probably attributed to the differences in the interaction strength and adsorption energy.[19,80] This is also reflected in the order of K_L values, which describes the intensity of the adsorption process (Table 3). Besides, from the fitting results with the Freundlich model, both K_F (representing the adsorption capacity) and n (representing the adsorption intensity) followed the same order of DMDBT > DBT > BT, further verifying the credence of the results.

Regeneration. For carbon sorbent in adsorptive desulfurization, the usually employed regeneration methods were solvent extraction[28,34,83] or thermal treatment.[83,84] In this work, we employed both methods as follows to investigate the regeneration performance of carbon sample C-2.

(a) Solvent extraction. After the first adsorption run (C_0 = 100 ppmwS DBT, T = 25 °C, adsorbent dosage = 2 g/L, no *para*-xylene added), the adsorbent was separated by centrifugation and then *para*-xylene was added (0.5 L/g). The mixture was ultrasonically treated using an ultrasonic cleaner for 1 h. After that, the adsorbent was separated by centrifugation again and dried at 145 °C overnight for the next adsorption run.

(b) Thermal treatment. After the first adsorption run, the adsorbent was separated by centrifugation, dried at 145 °C overnight and then heated at 500 °C in nitrogen atmosphere for 1 h for the next adsorption run.

As illustrated in Figure 8, the adsorbent regenerated by solvent extraction afforded 80% and 78% of the initial adsorption capacity for the second and the third run, whereas the corresponding values were 73% and 57% for the thermally regenerated sample. The regeneration efficiencies in our work are comparable to those of previously reported carbon adsorbents.[21,34,83,85]

Table S3 summarizes the DBT adsorption capacities over various adsorbents. The adsorption capacity over the activated sucrose-derived carbon (C-2) in our work is comparable or better than MOFs, ion-exchanged zeolites, graphene-like boron nitride and various carbon-based materials. Considering that higher initial concentrations generally lead to higher sulfur capacities,[34,71,86] a high adsorption capacity is expected if a higher initial concentration is employed. To address this issue, we further tested the ADS performance of C-2 at an initial concentration of 300 ppmwS DBT and achieved an increased q_{max} of 41.5 mgS/g (Figure S2). Combined with the fast adsorption rate, relatively good selectivity as well as potential for higher capacity and better selectivity with further post-treatment modifications (e.g., oxidation, incorporation of metals), the sucrose-derived activated carbon is considered a promising candidate for the removal of thiophenic compounds from transportation fuels.

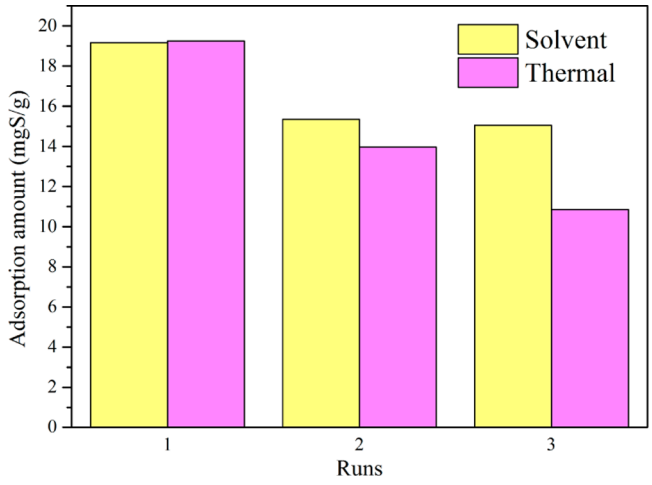

Figure 8. Regeneration performance of sample C-2 by solvent extraction or thermal regeneration (initial sulfur concentration: 100 ppmwS DBT, T = 25 °C, adsorbent dosage = 2 g/L, no *para*-xylene added).

Last but not least, the sucrose-derived activated carbon in the present work has several economic and environmental merits including the utilization of cheap natural precursor and low carbonization temperature. In the whole preparation process, no other solvent but water is used, preventing the possible environmental pollution caused by organic solvents. Moreover, the valuable potassium species may be recycled, which may further reduce the preparation cost (see details in the Supporting Information).

CONCLUSION

Activated carbons derived from hydrothermal carbonization of sucrose and subsequent KOH activation have been prepared and tested for the adsorptive removal of refractory thiophenic compounds (BT, DBT and DMDBT) from model fuels. The changes in textural and chemical properties of the carbons with an increase in the KOH/char ratio were characterized in detail by SEM, FTIR, nitrogen adsorption−desorption and CHN elemental analysis. On the basis of the kinetic studies, it was revealed that the adsorption rates were closely related to the mesopore fractions, whereas the adsorption amounts were related to the volumes of pores smaller than 1 nm as well as the contents of oxygen in the carbons. The adsorption isotherms were well fitted to the Langmuir and Freundlich models, and the maximum adsorption capacities were in the order of DMDBT > DBT > BT. The optimum carbon synthesized with a KOH/char ratio of 2 possessed a fast adsorption rate (97% saturated within 5 min), high adsorption capacity (41.5 mgS/g at C_0 = 300 ppmwS) and relatively good selectivity for the adsorption of thiophenic compounds. Combined with the economic and environmental merits of the preparation procedure, the sucrose-derived activated carbons may be promising candidates for potential practical applications.

DOI: 10.1021/acssuschemeng.5b00670
ACS Sustainable Chem. Eng. 2015, 3, 2237−2246

■ ASSOCIATED CONTENT

Supporting Information

The Supporting Information is available free of charge on the ACS Publications website at DOI: 10.1021/acssuschemeng.5b00670.

Comparison of HTC conditions as well as elemental compositions and yield of the sucrose-derived char produced by HTC with previous reports, details for BET analysis, further discussion on the recycle of potassium species, comparison of DBT adsorption capacity and adsorption isotherms over C-2 at initial sulfur concentration of 300 ppmwS (PDF).

■ AUTHOR INFORMATION

Corresponding Authors

*G. Liu. Tel./fax: +86 22 27892340. E-mail: gliu@tju.edu.cn.

*X. Zhang. Tel./fax: +86 22 27892340. E-mail: zhangxiangwen@tju.edu.cn

Notes

The authors declare no competing financial interest.

■ ACKNOWLEDGMENTS

Financial support from the National Natural Science Fund of China (U1232134) and Program for New Century Excellent Talents (NCET-13-0408) are gratefully acknowledged.

■ REFERENCES

(1) Song, C. An overview of new approaches to deep desulfurization for ultra-clean gasoline, diesel fuel and jet fuel. *Catal. Today* **2003**, *86* (1), 211−263.

(2) Chandra Srivastava, V. An evaluation of desulfurization technologies for sulfur removal from liquid fuels. *RSC Adv.* **2012**, *2* (3), 759−783.

(3) Zhu, W.; Dai, B.; Wu, P.; Chao, Y.; Xiong, J.; Xun, S.; Li, H.; Li, H. Graphene-analogue hexagonal BN supported with tungsten-based ionic liquid for oxidative desulfurization of fuels. *ACS Sustainable Chem. Eng.* **2015**, *3*, 186−194.

(4) Khan, N. A.; Jhung, S. H. Remarkable Adsorption Capacity of CuCl2-Loaded Porous Vanadium Benzenedicarboxylate for Benzothiophene. *Angew. Chem., Int. Ed.* **2012**, *51* (5), 1198−1201.

(5) Yu, C.; Fan, X.; Yu, L.; Bandosz, T. J.; Zhao, Z.; Qiu, J. Adsorptive Removal of Thiophenic Compounds from Oils by Activated Carbon Modified with Concentrated Nitric Acid. *Energy Fuels* **2013**, *27* (3), 1499−1505.

(6) Yang, R. T.; Hernandez-Maldonado, A. J.; Yang, F. H. Desulfurization of transportation fuels with zeolites under ambient conditions. *Science* **2003**, *301* (5629), 79−81.

(7) Ahmed, I.; Jhung, S. H. Composites of metal−organic frameworks: Preparation and application in adsorption. *Mater. Today* **2014**, *17* (3), 136−146.

(8) Palomino, J. M.; Tran, D. T.; Kareh, A. R.; Miller, C. A.; Gardner, J. M. V.; Dong, H.; Oliver, S. R. J. Zirconia-silica based mesoporous desulfurization adsorbents. *J. Power Sources* **2015**, *278*, 141−148.

(9) Velu, S.; Ma, X. L.; Song, C. S. Selective adsorption for removing sulfur from jet fuel over zeolite-based adsorbents. *Ind. Eng. Chem. Res.* **2003**, *42* (21), 5293−5304.

(10) Srivastav, A.; Srivastava, V. C. Adsorptive desulfurization by activated alumina. *J. Hazard. Mater.* **2009**, *170* (2−3), 1133−40.

(11) Li, W.; Tang, H.; Zhang, T.; Li, Q.; Xing, J.; Liu, H. Ultra-Deep Desulfurization Adsorbents for Hydrotreated Diesel with Magnetic Mesoporous Aluminosilicates. *AIChE J.* **2010**, *56* (5), 1391−1396.

(12) Xiao, J.; Wang, X.; Fujii, M.; Yang, Q.; Song, C. A Novel Approach for Ultra-Deep Adsorptive Desulfurization of Diesel Fuel over TiO_2-CeO_2/MCM-48 under Ambient Conditions. *AIChE J.* **2013**, *59* (5), 1441−1445.

(13) Kumar, S.; Srivastava, V. C.; Badoni, R. Studies on adsorptive desulfurization by zirconia based adsorbents. *Fuel* **2011**, *90* (11), 3209−3216.

(14) Cychosz, K. A.; Wong-Foy, A. G.; Matzger, A. J. Liquid phase adsorption by microporous coordination polymers: removal of organosulfur compounds. *J. Am. Chem. Soc.* **2008**, *130* (22), 6938−6939.

(15) Van de Voorde, B.; Bueken, B.; Denayer, J.; De Vos, D. Adsorptive separation on metal−organic frameworks in the liquid phase. *Chem. Soc. Rev.* **2014**, *43*, 5766−5788.

(16) Ania, C.; Bandosz, T. Metal-loaded polystyrene-based activated carbons as dibenzothiophene removal media via reactive adsorption. *Carbon* **2006**, *44* (12), 2404−2412.

(17) Seredych, M.; Lison, J.; Jans, U.; Bandosz, T. J. Textural and chemical factors affecting adsorption capacity of activated carbon in highly efficient desulfurization of diesel fuel. *Carbon* **2009**, *47* (10), 2491−2500.

(18) Yang, Y.; Lu, H.; Ying, P.; Jiang, Z.; Li, C. Selective dibenzothiophene adsorption on modified activated carbons. *Carbon* **2007**, *45* (15), 3042−3044.

(19) Wang, L.; Sun, B.; Yang, F. H.; Yang, R. T. Effects of aromatics on desulfurization of liquid fuel by π-complexation and carbon adsorbents. *Chem. Eng. Sci.* **2012**, *73*, 208−217.

(20) Shi, Y.; Zhang, X.; Wang, L.; Liu, G. MOF-derived porous carbon for adsorptive desulfurization. *AIChE J.* **2014**, *60* (8), 2747−2751.

(21) Shi, Y.; Liu, G.; Wang, L.; Zhang, X. Efficient adsorptive removal of dibenzothiophene from model fuel over heteroatom-doped porous carbons by carbonization of an organic salt. *Chem. Eng. J.* **2015**, *259*, 771−778.

(22) Wang, Q.; Liang, X.; Qiao, W.; Liu, C.; Liu, X.; Zhan, L.; Ling, L. Preparation of polystyrene-based activated carbon spheres with high surface area and their adsorption to dibenzothiophene. *Fuel Process. Technol.* **2009**, *90* (3), 381−387.

(23) Qiu, J.; Wang, G.; Bao, Y.; Zeng, D.; Chen, Y. Effect of oxidative modification of coal tar pitch-based mesoporous activated carbon on the adsorption of benzothiophene and dibenzothiophene. *Fuel Process. Technol.* **2015**, *129*, 85−90.

(24) Wu, L.; Sitamraju, S.; Xiao, J.; Liu, B.; Li, Z.; Janik, M. J.; Song, C. Effect of Liquid-phase O_3 Oxidation of Activated Carbon on the Adsorption of Thiophene. *Chem. Eng. J.* **2014**, *242*, 211−219.

(25) Yu, G. X.; Jin, M.; Sun, J.; Zhou, X. L.; Chen, L. F.; Wang, J. A. Oxidative modifications of rice hull-based carbons for dibenzothiophene adsorptive removal. *Catal. Today* **2013**, *212*, 31−37.

(26) Yu, M.; Li, Z.; Ji, Q.; Wang, S.; Su, D.; Lin, Y. S. Effect of thermal oxidation of activated carbon surface on its adsorption towards dibenzothiophene. *Chem. Eng. J.* **2009**, *148* (2−3), 242−247.

(27) Zhou, A.; Ma, X.; Song, C. Effects of oxidative modification of carbon surface on the adsorption of sulfur compounds in diesel fuel. *Appl. Catal., B* **2009**, *87* (3−4), 190−199.

(28) Zhou, A.; Ma, X.; Song, C. Liquid-phase adsorption of multi-ring thiophenic sulfur compounds on carbon materials with different surface properties. *J. Phys. Chem. B* **2006**, *110* (10), 4699−4707.

(29) Lan, P.; Zhang, S.; Pan, B.; Lv, L.; Zhang, W. Preparation and performance evaluation of resin-derived carbon spheres for desulfurization of fuels. *Sci. China: Chem.* **2013**, *56* (3), 393−398.

(30) Zhang, C.; Song, W.; Sun, G.; Xie, L.; Wan, L.; Wang, J.; Li, K. Synthesis, Characterization and Evaluation of Activated Carbon Spheres for Removal of Dibenzothiophene from Model Diesel Fuel. *Ind. Eng. Chem. Res.* **2014**, *53* (11), 4271−4276.

(31) Wang, L.; Yang, R. T.; Sun, C.-L. Graphene and other carbon sorbents for selective adsorption of thiophene from liquid fuel. *AIChE J.* **2013**, *59* (1), 29−32.

(32) Song, H. S.; Ko, C. H.; Ahn, W.; Kim, B. J.; Croiset, E.; Chen, Z.; Nam, S. C. Selective Dibenzothiophene Adsorption on Graphene Prepared Using Different Methods. *Ind. Eng. Chem. Res.* **2012**, *51* (30), 10259−10264.

(33) Anbia, M.; Parvin, Z. Desulfurization of fuels by means of a nanoporous carbon adsorbent. *Chem. Eng. Res. Des.* **2011**, *89* (6), 641−647.

DOI: 10.1021/acssuschemeng.5b00670
ACS Sustainable Chem. Eng. 2015, 3, 2237−2246

(34) Nejad, N. F.; Shams, E.; Amini, M. K.; Bennett, J. C. Ordered mesoporous carbon CMK-5 as a potential sorbent for fuel desulfurization: Application to the removal of dibenzothiophene and comparison with CMK-3. *Microporous Mesoporous Mater.* **2013**, *168*, 239−246.
(35) Ania, C.; Parra, J.; Arenillas, A.; Rubiera, F.; Bandosz, T.; Pis, J. On the mechanism of reactive adsorption of dibenzothiophene on organic waste derived carbons. *Appl. Surf. Sci.* **2007**, *253* (13), 5899−5903.
(36) Nunthaprechachan, T.; Pengpanich, S.; Hunsom, M. Adsorptive desulfurization of dibenzothiophene by sewage sludge-derived activated carbon. *Chem. Eng. J.* **2013**, *228*, 263−271.
(37) Sun, X.; Li, Y. Colloidal carbon spheres and their core/shell structures with noble-metal nanoparticles. *Angew. Chem., Int. Ed.* **2004**, *43* (5), 597−601.
(38) Titirici, M.-M.; White, R. J.; Falco, C.; Sevilla, M. Black perspectives for a green future: hydrothermal carbons for environment protection and energy storage. *Energy Environ. Sci.* **2012**, *5* (5), 6796.
(39) Romero-Anaya, A.; Ouzzine, M.; Lillo-Ródenas, M.; Linares-Solano, A. Spherical carbons: Synthesis, characterization and activation processes. *Carbon* **2014**, *68*, 296−307.
(40) Sevilla, M.; Fuertes, A. B.; Mokaya, R. High density hydrogen storage in superactivated carbons from hydrothermally carbonized renewable organic materials. *Energy Environ. Sci.* **2011**, *4* (4), 1400−1410.
(41) Titirici, M.-M.; Antonietti, M. Chemistry and materials options of sustainable carbon materials made by hydrothermal carbonization. *Chem. Soc. Rev.* **2010**, *39* (1), 103−116.
(42) Cui, X.; Antonietti, M.; Yu, S. H. Structural effects of iron oxide nanoparticles and iron ions on the hydrothermal carbonization of starch and rice carbohydrates. *Small* **2006**, *2* (6), 756−9.
(43) Wang, Q.; Li, H.; Chen, L.; Huang, X. Monodispersed hard carbon spherules with uniform nanopores. *Carbon* **2001**, *39* (14), 2211−2214.
(44) Zhao, L.; Fan, L. Z.; Zhou, M. Q.; Guan, H.; Qiao, S.; Antonietti, M.; Titirici, M. M. Nitrogen-Containing Hydrothermal Carbons with Superior Performance in Supercapacitors. *Adv. Mater.* **2010**, *22* (45), 5202−5206.
(45) Zhu, X.; Liu, Y.; Qian, F.; Zhou, C.; Zhang, S.; Chen, J. Role of Hydrochar Properties on the Porosity of Hydrochar-based Porous Carbon for Their Sustainable Application. *ACS Sustainable Chem. Eng.* **2015**, *3* (5), 833−840.
(46) Titirici, M.-M.; Antonietti, M.; Baccile, N. Hydrothermal carbon from biomass: a comparison of the local structure from poly-to monosaccharides and pentoses/hexoses. *Green Chem.* **2008**, *10* (11), 1204−1212.
(47) Sevilla, M.; Fuertes, A. B. Chemical and structural properties of carbonaceous products obtained by hydrothermal carbonization of saccharides. *Chem. - Eur. J.* **2009**, *15* (16), 4195−4203.
(48) Yu, L.; Falco, C.; Weber, J.; White, R. J.; Howe, J. Y.; Titirici, M.-M. Carbohydrate-derived hydrothermal carbons: a thorough characterization study. *Langmuir* **2012**, *28* (33), 12373−12383.
(49) Wang, J.; Kaskel, S. KOH activation of carbon-based materials for energy storage. *J. Mater. Chem.* **2012**, *22* (45), 23710.
(50) Wennerberg, A. N.; O'Grady, T. M. U.S. Patent 4,082,694, April 4, 1978.
(51) Sevilla, M.; Fuertes, A. B. Sustainable porous carbons with a superior performance for CO_2 capture. *Energy Environ. Sci.* **2011**, *4* (5), 1765−1771.
(52) Falco, C.; Marco-Lozar, J. P.; Salinas-Torres, D.; Morallón, E.; Cazorla-Amorós, D.; Titirici, M. M.; Lozano-Castelló, D. Tailoring the porosity of chemically activated hydrothermal carbons: Influence of the precursor and hydrothermal carbonization temperature. *Carbon* **2013**, *62*, 346−355.
(53) Mestre, A. S.; Tyszko, E.; Andrade, M. A.; Galhetas, M.; Freire, C.; Carvalho, A. P. Sustainable activated carbons prepared from a sucrose-derived hydrochar: remarkable adsorbents for pharmaceutical compounds. *RSC Adv.* **2015**, *5* (25), 19696−19707.
(54) Mao, L.; Zhang, Y.; Hu, Y.; Ho, K. H.; Ke, Q.; Liu, H.; Hu, Z.; Zhao, D.; Wang, J. Activation of sucrose-derived carbon spheres for high-performance supercapacitor electrodes. *RSC Adv.* **2015**, *5* (12), 9307−9313.
(55) Rouquerol, J.; Llewellyn, P.; Rouquerol, F. Is the BET equation applicable to microporous adsorbents? *Stud. Surf. Sci. Catal.* **2007**, *160*, 49−56.
(56) Enterría, M.; Suárez-García, F.; Martínez-Alonso, A.; Tascón, J. M. D. Synthesis of ordered micro−mesoporous carbons by activation of SBA-15 carbon replicas. *Microporous Mesoporous Mater.* **2012**, *151*, 390−396.
(57) Zheng, X.; Lv, W.; Tao, Y.; Shao, J.; Zhang, C.; Liu, D.; Luo, J.; Wang, D.-W.; Yang, Q.-H. Oriented and Interlinked Porous Carbon Nanosheets with an Extraordinary Capacitive Performance. *Chem. Mater.* **2014**, *26* (23), 6896−6903.
(58) Sevilla, M.; Mokaya, R. Energy storage applications of activated carbons: supercapacitors and hydrogen storage. *Energy Environ. Sci.* **2014**, *7* (4), 1250−1280.
(59) Sevilla, M.; Fuertes, A. B. A general and facile synthesis strategy towards highly porous carbons: carbonization of organic salts. *J. Mater. Chem. A* **2013**, *1* (44), 13738−13741.
(60) Figueiredo, J.; Pereira, M.; Freitas, M.; Orfao, J. Modification of the surface chemistry of activated carbons. *Carbon* **1999**, *37* (9), 1379−1389.
(61) Sun, C.; Xu, D.; Xue, D. Direct in situ ATR-IR spectroscopy of structural dynamics of NH_4H_2PO4 in aqueous solution. *CrystEngComm* **2013**, *15* (38), 7783.
(62) Titirici, M. M. *Sustainable Carbon Materials from Hydrothermal Processes*; Wiley: West Sussex, U. K., 2013.
(63) Adeniran, B.; Masika, E.; Mokaya, R. A family of microporous carbons prepared via a simple metal salt carbonization route with high selectivity for exceptional gravimetric and volumetric post-combustion CO_2 capture. *J. Mater. Chem. A* **2014**, *2*, 14696−14710.
(64) Shiratori, N.; Lee, K. J.; Miyawaki, J.; Hong, S. H.; Mochida, I.; An, B.; Yokogawa, K.; Jang, J.; Yoon, S. H. Pore structure analysis of activated carbon fiber by microdomain-based model. *Langmuir* **2009**, *25* (13), 7631−7.
(65) Yang, T.; Lua, A. C. Characteristics of activated carbons prepared from pistachio-nut shells by potassium hydroxide activation. *Microporous Mesoporous Mater.* **2003**, *63* (1−3), 113−124.
(66) Arcibar-Orozco, J. A.; Rangel-Mendez, J. R.; Bandosz, T. J. Desulfurization of Model Diesel Fuel on Activated Carbon Modified with Iron Oxyhydroxide Nanoparticles: Effect oftert-Butylbenzene and Naphthalene Concentrations. *Energy Fuels* **2013**, *27* (9), 5380−5387.
(67) Seredych, M.; Bandosz, T. J. Selective adsorption of dibenzothiophenes on activated carbons with Ag, Co, and Ni species deposited on their surfaces. *Energy Fuels* **2009**, *23* (7), 3737−3744.
(68) Seredych, M.; Bandosz, T. J. Effect of the graphene phase presence in nanoporous S-doped carbon on photoactivity in UV and visible light. *Appl. Catal., B* **2014**, *147*, 842−850.
(69) Zhang, W.; Liu, H.; Xia, Q.; Li, Z. Enhancement of dibenzothiophene adsorption on activated carbons by surface modification using low temperature oxygen plasma. *Chem. Eng. J.* **2012**, *209*, 597−600.
(70) Han, X.; Lin, H.; Zheng, Y. Adsorptive denitrogenation and desulfurization of diesel using activated carbons oxidized by $(NH_4)_2S_2O_8$ under mild conditions. *Can. J. Chem. Eng.* **2015**, *93*, 538−548.
(71) Xiong, J.; Zhu, W.; Li, H.; Ding, W.; Chao, Y.; Wu, P.; Xun, S.; Zhang, M.; Li, H. Few-layer Graphene-like Boron Nitride Induced Remarkable Adsorption Capacity for Dibenzothiophene in Fuels. *Green Chem.* **2015**, *17*, 1647−1656.
(72) Jia, S. Y.; Zhang, Y. F.; Liu, Y.; Qin, F. X.; Ren, H. T.; Wu, S. H. Adsorptive removal of dibenzothiophene from model fuels over one-pot synthesized PTA@MIL-101(Cr) hybrid material. *J. Hazard. Mater.* **2013**, *262*, 589−97.
(73) Xu, C.; Guan, J.; Wu, S.; Jia, M.; Wu, T.; Kan, Q. Catalytic performance of zeolite ITQ-13 with 9-and 10-member rings for methane dehydroaromation. *React. Kinet., Mech. Catal.* **2010**, *99* (1), 193−199.

DOI: 10.1021/acssuschemeng.5b00670
ACS Sustainable Chem. Eng. 2015, 3, 2237−2246

(74) Gui, P.; Li, X.; Zhang, S.; Xu, Q.; Dou, T. Quasi-solid state synthesis of EU-1 zeolite and its catalytic properties for the isomerization of C8 aromatics. *Pet. Sci.* **2012**, *9* (4), 544−550.
(75) Shi, F.; Hammoud, M.; Thompson, L. T. Selective adsorption of dibenzothiophene by functionalized metal organic framework sorbents. *Appl. Catal., B* **2011**, *103* (3−4), 261−265.
(76) Seredych, M.; Hulicova-Jurcakova, D.; Bandosz, T. J. Effect of the incorporation of nitrogen to a carbon matrix on the selectivity and capacity for adsorption of dibenzothiophenes from model diesel fuel. *Langmuir* **2010**, *26* (1), 227−33.
(77) Zhou, H.; Li, G.; Wang, X.; Jin, C.; Chen, Y. Preparation of a kind of mesoporous carbon and its performance in adsorptive desulfurization. *J. Nat. Gas Chem.* **2009**, *18* (3), 365−368.
(78) Fallah, R. N.; Azizian, S.; Reggers, G.; Carleer, R.; Schreurs, S.; Ahenach, J.; Meynen, V.; Yperman, J. Effect of aromatics on the adsorption of thiophenic sulfur compounds from model diesel fuel by activated carbon cloth. *Fuel Process. Technol.* **2014**, *119*, 278−285.
(79) Fallah, R. N.; Azizian, S. Removal of thiophenic compounds from liquid fuel by different modified activated carbon cloths. *Fuel Process. Technol.* **2012**, *93* (1), 45−52.
(80) Xiao, J.; Song, C.; Ma, X.; Li, Z. Effects of Aromatics, Diesel Additives, Nitrogen Compounds, and Moisture on Adsorptive Desulfurization of Diesel Fuel over Activated Carbon. *Ind. Eng. Chem. Res.* **2012**, *51* (8), 3436−3443.
(81) Tang, H.; Li, W.; Zhang, T.; Li, Q.; Xing, J.; Liu, H. Improvement in diesel desulfurization capacity by equilibrium isotherms analysis. *Sep. Purif. Technol.* **2011**, *78* (3), 352−356.
(82) Kim, J. H.; Ma, X. L.; Zhou, A. N.; Song, C. S. Ultra-deep desulfurization and denitrogenation of diesel fuel by selective adsorption over three different adsorbents: A study on adsorptive selectivity and mechanism. *Catal. Today* **2006**, *111* (1−2), 74−83.
(83) Han, X.; Lin, H.; Zheng, Y. Regeneration methods to restore carbon adsorptive capacity of dibenzothiophene and neutral nitrogen heteroaromatic compounds. *Chem. Eng. J.* **2014**, *243*, 315−325.
(84) Seredych, M.; Rawlins, J.; Bandosz, T. J. Investigation of the Thermal Regeneration Efficiency of Activated Carbons Used in the Desulfurization of Model Diesel Fuel. *Ind. Eng. Chem. Res.* **2011**, *50* (24), 14097−14104.
(85) Wang, Y.; Yang, R. T. Desulfurization of liquid fuels by adsorption on carbon-based sorbents and ultrasound-assisted sorbent regeneration. *Langmuir* **2007**, *23* (7), 3825−3831.
(86) Shen, C.; Wang, Y. J.; Xu, J. H.; Lu, Y. C.; Luo, G. S. Porous glass beads as a new adsorbent to remove sulfur-containing compounds. *Green Chem.* **2012**, *14* (4), 1009−1015.

DOI: 10.1021/acssuschemeng.5b00670
ACS Sustainable Chem. Eng. 2015, 3, 2237−2246